The Astrophysical Journal, 651:1245–1255, 2006 November 10

A STUDY OF THE ORIENTATION OF INTERPLANETARY MAGNETIC CLOUDS AND SOLAR FILAMENTS

Yuming Wang,[1,2] Guiping Zhou,[3] Pinzhong Ye,[1] S. Wang,[1] and Jingxiu Wang[3]
Received 2005 July 25; accepted 2006 July 13

ABSTRACT

As a kind of eruptive phenomenon associated with coronal mass ejections (CMEs), solar eruptive filaments are thought to be parallel to the axis of surrounding arcade coronal magnetic fields that erupt and develop into interplanetary magnetic clouds (MCs). By investigating three events from 2000 August, 2003 October, and 2003 November, we estimate the axial orientations of the MCs and make a quantitative comparison with the filament orientations. By defining "tilt angle" as the angle between projected orientation on the plane of the sky and the ecliptic, we find that the tilt angles of these MCs are about 30°, 60°, and 55°, respectively. However, Hα images show that the associated filaments were all highly curved. The tilt angles of the long axes of these filaments prior to their eruption vary in a range that corresponds to tangents along the entire curved path of the filaments. Comparison between the MCs and filaments shows that for the first and third events, the estimated MC tilt angles are within the range of tilt angles of the associated filaments and almost parallel to the central parts of the filaments. But for the second event, the MC tilt angle is outside the range. This work suggests that (1) the curvature of filaments should be considered in studying the relation between filament and MC orientations, (2) inconsistencies between them do occur, even if the filament curvature is taken into account, and (3) the largest deviation in the tilt angle between MCs and their associated filaments occurs for those MCs whose orientations are not perpendicular to the Earth-Sun line, indicating that the measured part of the MC is not its leading front.

Subject headings: solar-terrestrial relations — Sun: coronal mass ejections (CMEs) — Sun: filaments

1. INTRODUCTION

In the current paradigm, filament-associated magnetic clouds (MCs) are thought to be the result of sheared coronal loops surrounding the filament, which develop into a flux rope–like structure through magnetic field reconnection (see, e.g., Gosling et al. 1995; Martin & McAllister 1997; Filippov 1998). Figure 1 depicts the widely accepted geometry of MCs (taken from Marubashi 1997). Although MCs are curved structures on a large scale, the projection of the axis of an MC on the plane of the sky, especially the central part—that is, the leading front, as denoted by the shaded regions in Figure 1—should roughly align with the long axis of the associated filament prior to eruption. This view is supported by many previous works (e.g., Bothmer & Schwenn 1994; Bothmer & Rust 1997; Marubashi 1997; McAllister et al. 2001; Yurchyshyn et al. 2001), which also suggest that the sign of the helicity (or handedness) of MCs should be in agreement with the chirality of the coronal arcades overlying the associated filaments. A direct application of this idea is the prediction of geomagnetic storms caused by MCs, as applied by McAllister et al. (2001) and Jing et al. (2004).

Geomagnetic storms are one of the most important processes affecting the plasma environment around Earth. Large nonrecurrent geomagnetic storms are mainly caused by coronal mass ejections (CMEs), nearly half of which contain MCs (Gosling et al. 1992; Cane et al. 1997; Burlaga et al. 2001), and shock sheaths that precede them (e.g., Sheeley et al. 1985; Gosling et al. 1991). Over the past several decades, the relationship between interplanetary solar wind parameters and the intensities of geomagnetic storms has been studied extensively (e.g., Burton et al. 1975; Perreault & Akasofu 1978; Gonzalez & Tsurutani 1987; Gonzalez et al. 1989; Tsurutani & Gonzalez 1995; Wang et al. 2003a). The intensity of a geomagnetic storm now can be predicted fairly well on a real-time basis using near-Earth solar wind data. Even so, longer term predictions are still looked forward to. Here, "longer term" means a prediction made based on solar eruptions, which usually take place several days before the subsequent storm. For an MC-caused geomagnetic storm, the cloud's axial orientation will significantly affect the storm intensity. So, if the correlation between MCs and filaments mentioned above is strong, a longer term prediction of MC-caused geomagnetic storms might be possible.

Nevertheless, there are other problems with the longer term prediction of MC-caused geomagnetic storms. Not all CMEs develop into magnetic clouds (Richardson & Cane 2004). The association of solar eruptive events with MCs is not straightforward (Berdichevsky et al. 2005). The speed of MCs varies over a large range, so that the arrival time of an MC is not easy to predict. A full investigation of these problems is beyond the scope of this paper. What we focus on here is whether some properties of the magnetic field configuration of MCs can be deduced from the eruptive filaments seen on the Sun, and to what extent useful predictions of magnetic cloud orientation can be made by measuring the orientations of the associated filaments prior to their eruption.

In most reported studies, the MC orientation and handedness are consistent with the associated eruptive structures. However, exceptions do exist. Rust et al. (2005) reported that the axial orientation of two out of six flux ropes they studied did not agree with that of the associated filaments or sigmoids. Moreover, most filaments are curved on the surface of the Sun. In papers to date, a straight line between the filament endpoints has been used as a first-order approximation to represent the filament's axis. This raises uncertainties in predicting the MC's orientation and should

[1] School of Earth and Space Sciences, University of Science and Technology of China, 96 Jinzhai Road, Hefei, 230026 Anhui, China; ymwang@ustc.edu.cn.
[2] College of Science, George Mason University, 4400 University Drive, MSN 6A2, Fairfax, VA 22030.
[3] National Astronomical Observatories of China, 20A Datun Road, 100012 Beijing, China.

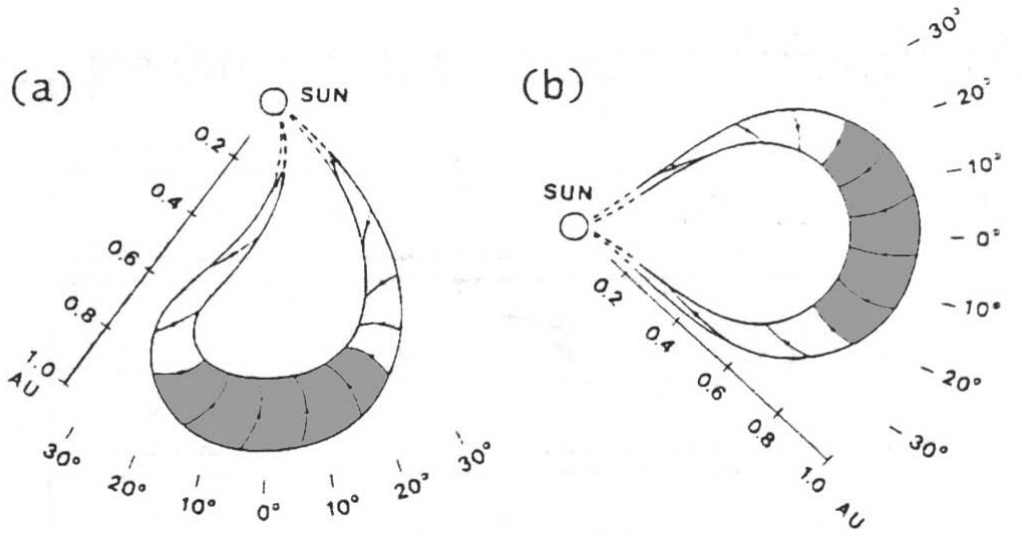

FIG. 1.—Sketch illustrating the geometry of interplanetary MCs (from Marubashi 1997). The central parts, i.e., the leading fronts, of the MCs are indicated by shaded regions.

be taken into account. Thus, in this paper we perform a more careful and quantitative study of this topic.

2. OBSERVATIONS AND RESULTS

A typical MC usually has three signatures, as proposed by Burlaga et al. (1981): enhanced magnetic field strength, a large and smooth rotation of the magnetic field vector, and low proton temperature and β. Based on observations of the solar wind plasma and magnetic field from the *Advanced Composition Explorer* (*ACE*) spacecraft at 1 AU, we selected magnetic clouds associated with large geomagnetic storms. By examining CME observations from the Large Angle and Spectrometric Coronagraph (LASCO; Brueckner et al. 1995) and coronal observations from the Extreme-Ultraviolet Imaging Telescope (EIT; Delaboudinière et al. 1995) on board the *Solar and Heliospheric Observatory* (*SOHO*), we identified CMEs and eruptive filaments associated with the magnetic clouds. The criteria used in selecting events are that (1) there is only one filament in the CME source region, in other words, no complex filament system around it; (2) the filament is large and dark, that is, it must be seen clearly in Hα images; and (3) there is sufficient Hα data coverage to display the filament's disappearance. By applying these rules, three events were selected. The analysis of these events is described below.

2.1. *2000 August Event*

Figure 2 shows the observations of a magnetic cloud that passed Earth during 2000 August 12–13. Its boundaries are indicated by the vertical dashed lines, within which the signatures of the MC are evident. The magnetic field strength was enhanced to about 35 nT. The elevation angle of the magnetic field vector rotated from roughly -90° to 90°, and the change in azimuthal angle was negligible. The solar wind speed decreased, suggesting an expanding structure. The proton temperature and β were both significantly lower than those in the ambient solar wind. A β-value less than 0.1 is a good indicator of an MC (Farrugia et al. 1993; Tsurutani & Gonzalez 1995). This MC drove a shock, followed by a 12 hr shock sheath, at 18:09 UT on August 11.

Cliver et al. (1990) established a relationship between the average speed of travel, V_t, of an interplanetary shock from the Sun to 1 AU and the in situ maximum solar wind speed, $V_{\max}$, behind the shock for interplanetary ejecta:

$$V_{\max} \approx 0.775 V_t - 40 \text{ km s}^{-1}. \quad (1)$$

With the aid of this relationship, we can estimate the onset t_0 of the CME corresponding to this MC and then search for it within a reasonable time window. This method was used in our previous work (Wang et al. 2002b, 2003b). Here we choose a window of 12 hr centered on t_0. From Figure 2, the value of $V_{\max}$ for this event was approximately 650 km s^{-1}, and therefore $V_t \sim 890$ km s^{-1}. This speed corresponds to a 46.8 hr travel time from the Sun to 1 AU. The related CME should have occurred near 19:20 UT on August 9. The LASCO CME Catalog[4] was used to select CME candidates. We consider only halo CMEs whose apparent width in LASCO is larger than 130° (e.g., Hudson et al. 1998; Wang et al. 2002b).

The catalog shows that there was only one CME in the time window of interest. It is a full-halo CME that first appeared in the LASCO C2 camera at 16:30 UT on August 9. Figure 3*a* displays a combined image of the eruption and propagation of this CME as seen in EIT and LASCO. This CME traveled along the northeast direction in the plane of the sky. Before the CME appeared in the C2 image, a filament eruption occurred, as shown in the EIT images. Figure 3*b* exhibits an evident rapid rising of filament material from 16:11 to 16:35 UT. The time and direction viewed in the EIT images are consistent with those viewed in the LASCO image. Figure 3*c* shows the Hα images from Big Bear Solar Observatory (BBSO) before and after the eruption. The filament, as marked by the circles, disappeared after the eruption. We thus conclude that this was a front-side CME related to the filament eruption and is the source of the MC observed near Earth during August 12–13.

To compare the magnetic field configuration of the MC with the associated filament and its overlying coronal arcades, we adopt a force-free flux rope model of MCs (e.g., Goldstein 1983; Burlaga

[4] See http://cdaw.gsfc.nasa.gov/CME_list, which is generated and maintained at the CDAW Data Center by NASA and the Catholic University of America in cooperation with the Naval Research Laboratory.

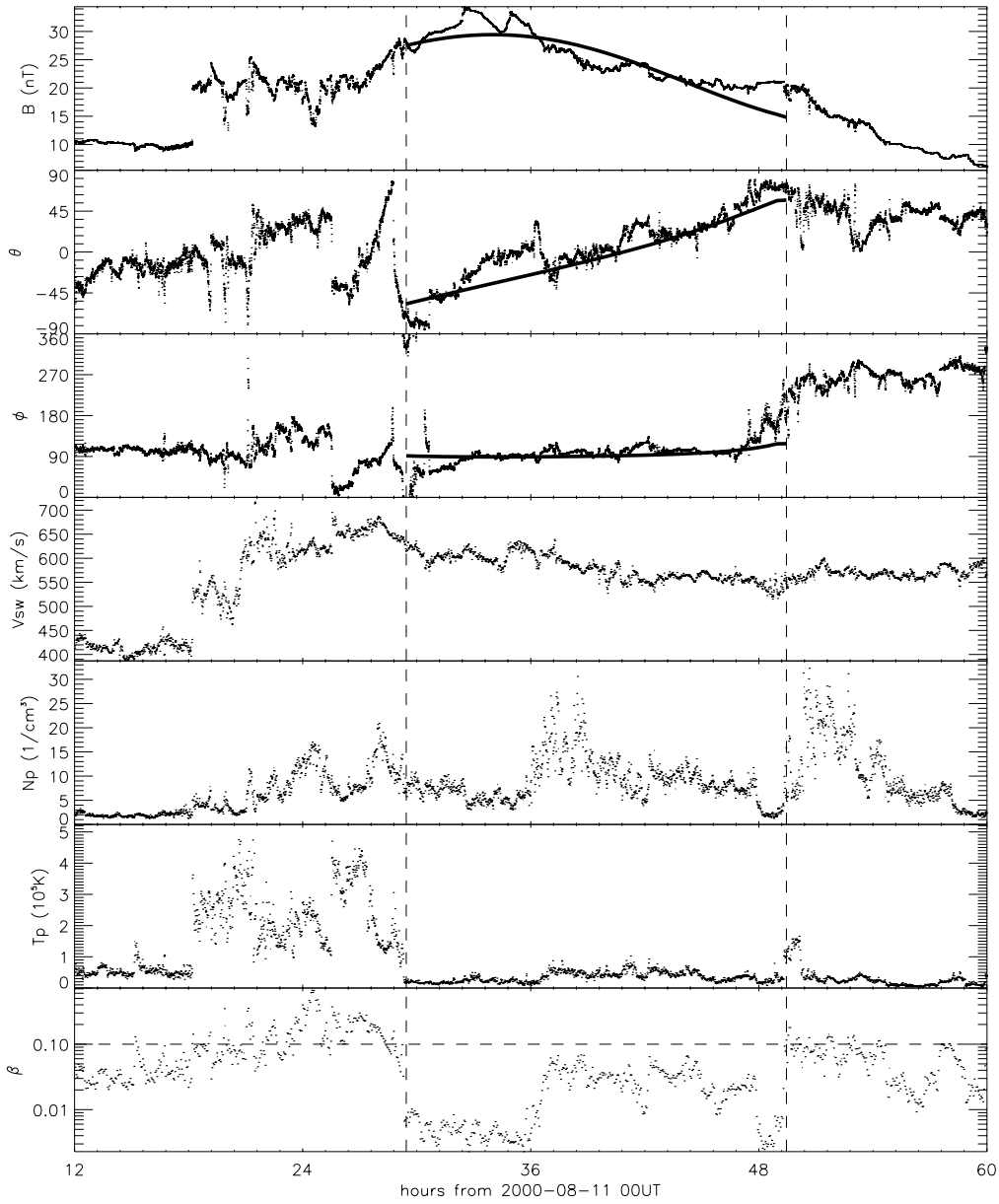

FIG. 2.—*ACE* magnetic field and solar wind plasma observations of the 2000 August event (in GSE coordinates). From top to bottom are plotted magnetic field strength B, the elevation θ and azimuthal ϕ angles of magnetic field direction, solar wind speed V_{sw}, the proton number density N_p and temperature T_p, and the plasma β.

1988; Lepping et al. 1990; Kumar & Rust 1996), which is given by the Lundquist (1950) solution in cylindrical coordinates (R, Φ, Z):

$$B_R = 0, \quad B_\Phi = HB_0 J_1(\alpha R), \quad B_Z = B_0 J_0(\alpha R), \qquad (2)$$

where $H = \pm 1$ indicates the sign of the helicity, B_0 is the magnetic field strength at the axis, and J_0 and J_1 are Bessel functions of orders 0 and 1, respectively. As in our previous work (Wang et al. 2002a, 2003b), we use the flux rope model to fit the MC, from which seven parameters are obtained (see cols. [4]–[11] of Table 1 for interpretation). For this MC, the fitted curves are plotted over the observed magnetic field profiles in the top three panels of Figure 2. The normalized rms deviation and correlation coefficient are 0.1 and 0.92, respectively, which indicate a good match to the observations. The sign of the helicity of this MC was negative. The estimated axial orientation of this MC was $\theta \sim -29^\circ$ and $\phi \sim 73^\circ$ in geocentric solar ecliptic (GSE) coordinates. Defining "tilt angle" as the angle between projected orientation on the plane of the sky and the ecliptic plane, we infer that the tilt angle of the MC axis was $\sim 30^\circ$. It can also be inferred that the angle between the MC axis and the Sun-Earth line was $\sim 75^\circ$, indicating that the axis was nearly perpendicular to the Sun-Earth line. According to the geometry illustrated in Figure 1, a perpendicular MC axis implies that the leading front of the cloud was measured.

Figure 4 is an Hα image overplotted with the contours of the magnetogram from the *SOHO* Michelson Doppler Imager (MDI). The yellow contours denote positive polarity, and the green contours indicate negative polarity. The blue arrows from positive to negative indicate coronal arcades overlying the filament. One can see that the erupted filament was largely curved. Its upper right part was in the east-west direction, and its lower left part was almost in the north-south direction. Because of the curved shape, the tilt angle of the long axis of the filament varies in a range that corresponds to tangents along the entire curved path of the filament. In this case, it was from about 0° to 75°, as marked

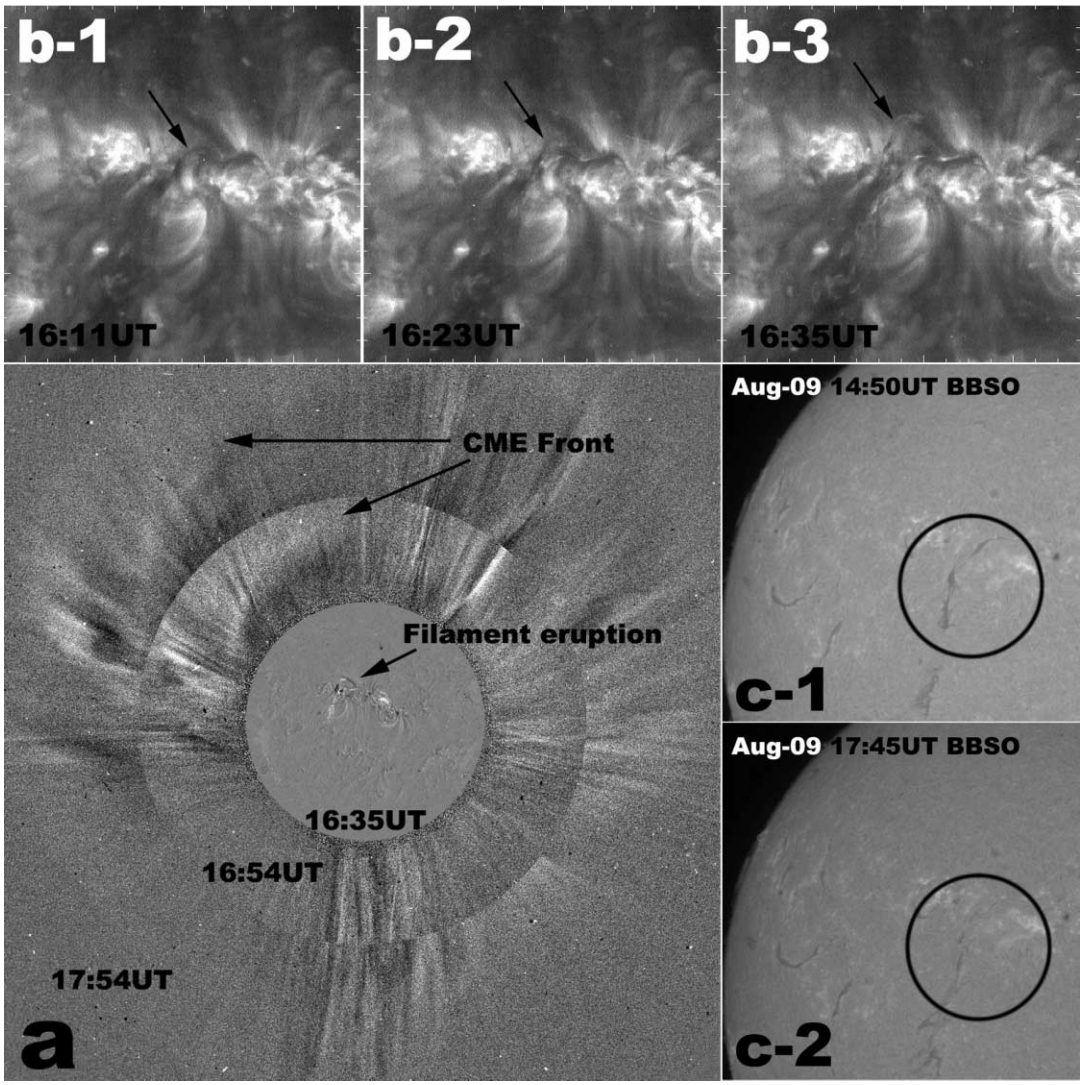

FIG. 3.—Observations of the 2000 August 9 CME and related solar activity. (*a*) A combined running-difference LASCO C2 image, in which the occulting disk is filled in with an enlarged running-difference EIT 195 Å image. It clearly displays the CME and its source region. (*b*) Three consecutive EIT 195 Å images showing filament eruption. (*c*) Two Hα images, taken before and after the eruption, indicating the disappearance of the filament.

TABLE 1

SUMMARY OF THE MAGNETIC CLOUDS AND THEIR ASSOCIATED DISAPPEARING FILAMENTS

	OBSERVED MC		FITTED PARAMETERS								ASSOCIATED FILAMENT		
No.	Date	T[a]	B_0[b]	H[c]	θ[d]	ϕ[d]	t_c[e]	R_0[f]	D/R_0[g]	χ^2/c.c.[h]	Date/Time[i]	Location	Tilt[j]
(1)	(2)	(3)	(4)	(5)	(6)	(7)	(8)	(9)	(10)	(11)	(12)	(13)	(14)
1.....	2000 Aug 12–13	5.2–25.0	30.9	−1	−29	73	10	14	−0.17	0.10/0.92	2000 Aug 9, 16:30	N20, E15	0° to 75° (30°)
2.....	2000 Oct 13–14	16.8–29.4	12.6	1	−52	47	22	13	0.33	0.02/0.99	2000 Oct 9, 23:50	N02, W06	−15° to 30° (60°)
3.....	2003 Nov 20–21	10.1–24.4	50.0	1	−55	90	15	7	0.00	0.09/0.93	2003 Nov 18, 08:50	N03, E18	−25° to 110° (55°)

[a] Start and end times of the observed MC (in hours).
[b] Magnetic field magnitude at the axis of the flux rope (in nT).
[c] Sign of the helicity, i.e., handedness.
[d] Elevation (θ) and azimuthal (ϕ) angle of the axial field (i.e., the orientation of the axis) of the flux rope in GSE coordinates.
[e] Center time at the closest distance of the spacecraft's trajectory to the axis (in hours from the beginning of the day).
[f] Flux rope radius (in hours).
[g] Closest distance to the rope axis (in hours). $D > 0$ means that the axis is above the spacecraft's trajectory.
[h] Goodness of fit: rms deviation and correlation coefficient.
[i] First appearance of the related CME in LASCO C2.
[j] Range of the filiament tilt angle. The value in parentheses denotes the tilt angle of the related MC's axis.

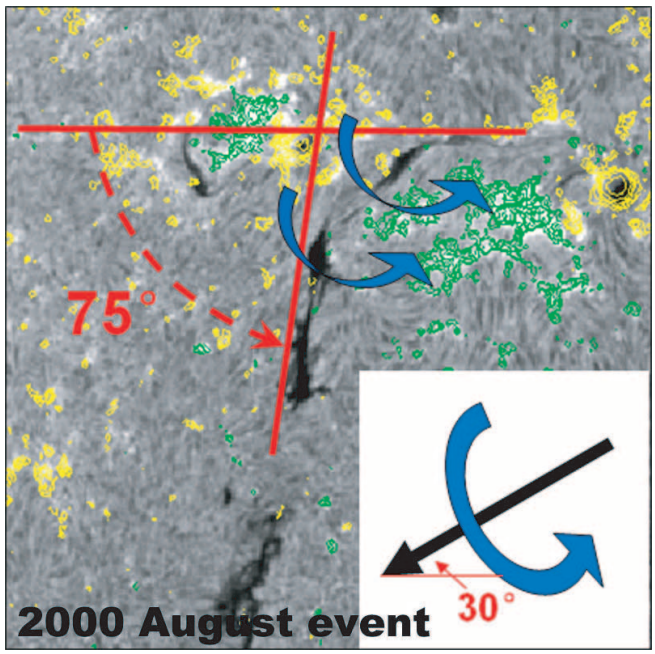

FIG. 4.—Hα image of the 2000 August event, overplotted with contours from the *SOHO* MDI magnetogram, in which yellow denotes positive polarity and green denotes negative polarity. The blue arrows from positive to negative indicate coronal arcades overlying the filament. The red lines mark the range of the direction of the filament, which was $\sim 75^\circ$ for this case, indicating a significantly curved filament. For comparison, the projected axis of the related MC on the sky plane is shown at lower right.

by the red lines and dashed red arrow. The orientation (projected onto the plane of the sky; i.e., tilt angle) of the related MC axis is plotted at lower right in Figure 4. According to the parameters of the MC inferred in the previous paragraph, the tilt angle of the MC axis was $\sim 30^\circ$. It was within the span of the filament direction and almost parallel to the central part of the filament. Moreover, the rotational direction of the helical magnetic field lines in this MC was the same as that of the coronal arcades overlying the filament.

2.2. *2000 October Event*

The interplanetary magnetic field and solar wind plasma observations of the 2000 October event are shown in Figure 5. Obviously, an MC was passing through the *ACE* spacecraft from 16:48 UT on October 13 to 05:24 UT the next day. The discontinuities at the boundaries are very clear. The magnetic field direction rotated significantly and smoothly during this period, although the enhancement of the magnetic field strength was not so strong. Meanwhile, the solar wind speed decreased continuously, the proton temperature dropped to a low value, and the value of the proton β was less than 0.1. Thus, this structure was clearly an MC. The solar wind profile shows that this MC was too slow to drive a shock ahead of it.

Since there was no shock, we do not use equation (1) to estimate the source CME. This MC was a slow one, so we searched for the CME in a reasonably large interval from October 9 to 11. The LASCO CME Catalog shows there were only two halo CMEs during this period. One was a full-halo CME first appearing at 23:50 UT on October 9, and the other was a partial-halo CME with an angular width of 228° that first appeared at 06:50 UT on October 11.

The LASCO and EIT observations for the former CME are shown in Figure 6. The combined LASCO-EIT image (Fig. 6*a*) demonstrates a definite association between the activity on the solar surface and this CME. The running-difference EIT image displays the corona at 23:35 UT on October 9, which reveals an evident eruption. The eruption propagated into the field of view of LASCO C2, as shown in the two LASCO snapshots from the next day. The eruption observed by EIT was consistent with the CME observed by LASCO in both time and space. The EIT snapshots (Fig. 6*b*) show the process of this eruption in more detail. It began at about 23:11 UT and formed posteruption loops at approximately 00:47 UT. Hα observations of the same region also show a filament disappearance (Fig. 6*c*). The Hα image from BBSO in the upper panel of Figure 6*c* was taken at 16:31 UT. The region marked by the oval is where the CME originated. One can note that there was a filament. The Hα image from the Yunnan Astronomical Observatory (YNAO) in the lower panel was taken at 03:16 UT on October 10. It is clear that, in the same marked region, the filament had erupted. Thus, this halo CME was front-side and related to a filament eruption. For the partial-halo CME that appeared at 06:50 UT on October 11, we also examined the EIT movies carefully but found no evident eruption near that time. This CME was likely from the back side of the Sun. Thus, the source of the MC observed at 1 AU should be the filament-associated CME that occurred at 23:50 UT on October 9.

Similarly, we use the flux rope model to fit the observed MC. The fitted curves are plotted in the top three panels of Figure 5, and the fitted parameters are listed in Table 1. The results suggest that this MC had positive helicity and its axis pointed to $\theta \sim -52^\circ$ and $\phi \sim 47^\circ$. The angle between the axis and the Sun-Earth line was $\sim 65^\circ$. This value implies that the spacecraft did not pass right through the leading front of the MC. By projecting the MC axis onto the plane of the sky, the tilt angle can be inferred to be approximately 60°.

Figure 7 shows the comparison between this MC and the related filament. From the Hα image, one can observe that this filament was curved and its tilt angle varied from about -15° to 30°. According to the photospheric magnetogram, the coronal field lines overlying the filament pointed approximately from south to north. Compared with the filament and the coronal magnetic field surrounding it, the axial orientation of this MC was not within the range of the filament's direction. It was about 30° above the upper limit of the filament direction.

2.3. *2003 November Event*

This is a well-known event that caused an extremely large geomagnetic storm (see, e.g., Ermolaev et al. 2005). Figure 8 shows the interplanetary magnetic field and solar wind plasma observations of this event. Evidently, a magnetic cloud was passing through Earth from 10:06 UT on November 20 until the end of that day, as denoted by the two vertical dashed lines. Within this period, the signatures of a typical MC are all clear: enhanced magnetic field (up to 56 nT), long smooth rotation of the magnetic field direction, declining solar wind speed, low proton temperature, and low β (<0.1). Because of its rapid motion, a shock was driven ahead at 07:27 UT.

From the solar wind profile in Figure 8, we estimate the value of $V_{\max}$ to be ~ 750 km s^{-1}, and therefore V_t is approximately 1019.4 km s^{-1} according to equation (1). So, the travel time of the shock was about 40.9 hr, indicating that the onset of the source CME should have been near 14:33 UT on November 18. By searching in a reasonable time window of 12 hr in the LASCO CME Catalog, we find that there are two possible CMEs. One was a full-halo CME first appearing at 08:50 UT on November 18, and the other was a partial-halo CME with an angular width larger than 197° that first appeared at 09:50 UT the same day.

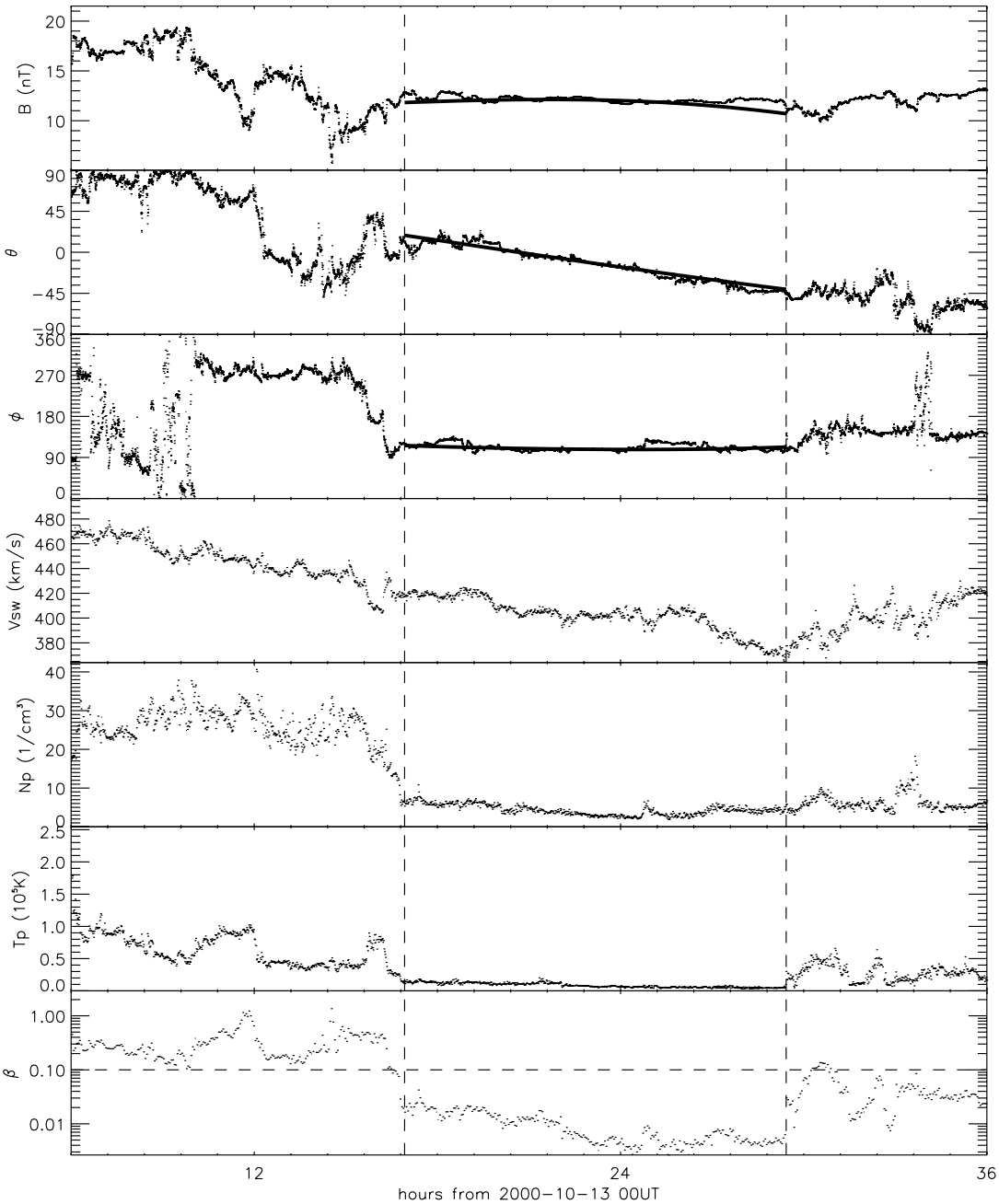

FIG. 5.—Same as Fig. 2, but for the 2000 October event.

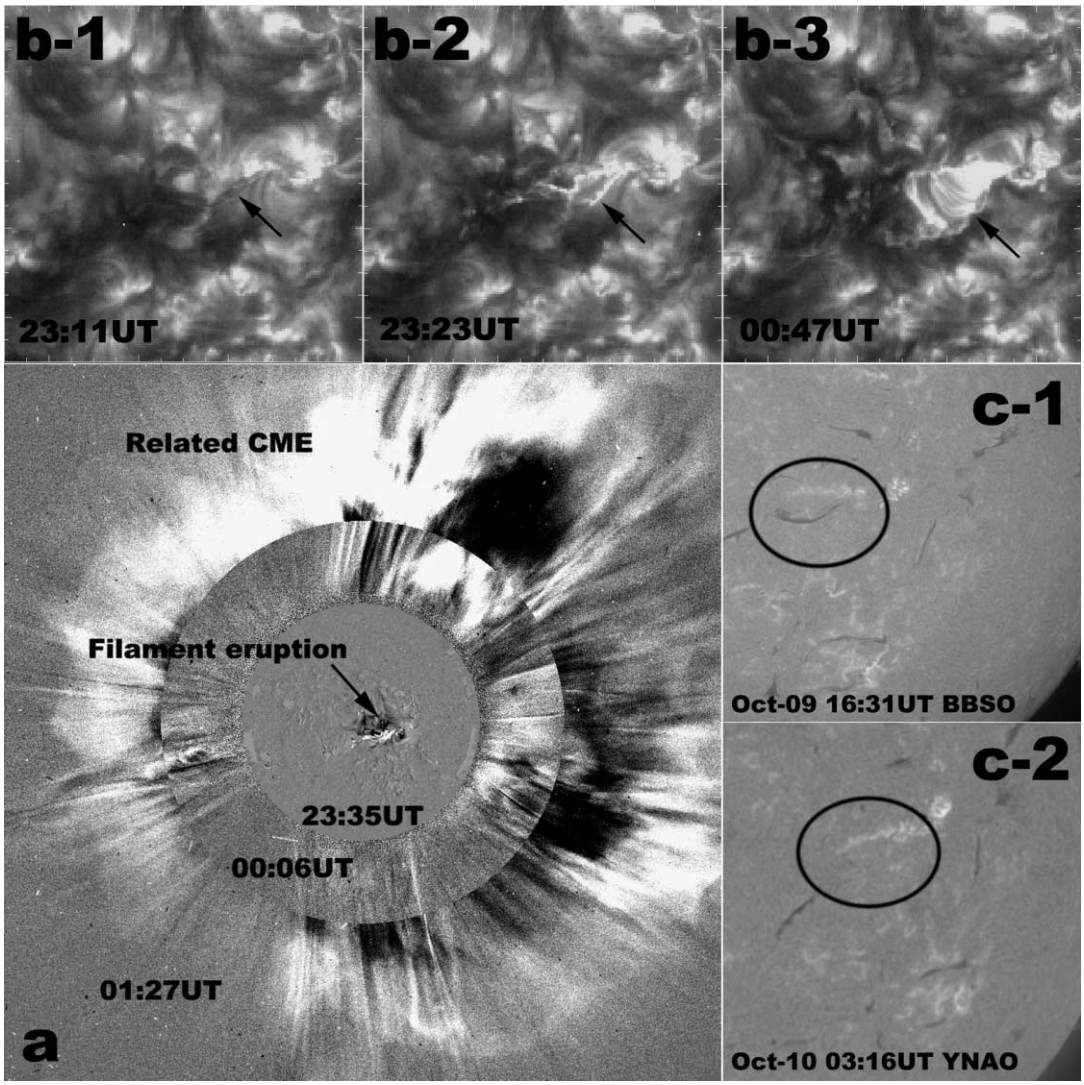

FIG. 6.—Same as Fig. 3, but for the 2000 October 9 CME and related solar activity.

By checking the EIT data, the later partial CME turns out not to have been a front-side event. It originated from the east limb. Since it was very fast (projected speed near 2000 km s^{-1}), it would not have encountered Earth (Wang et al. 2004, 2006). Thus, the only candidate to have been responsible for the MC observed at 1 AU is the former CME. Figure 9 displays the solar observations of this CME. The combined LASCO-EIT image (Fig. 9*a*) reveals the propagation of the eruption process from the solar surface to several solar radii. The EIT image clearly reveals the location of the source region and the front of this eruption. The two LASCO C2 snapshots show that a CME propagated in the same direction following the EIT eruption. The three EIT images (Fig. 9*b*) reveal that this eruption began from the east end of a filament at 07:12 UT and then extended to the entire filament region. Near 10:46 UT, posteruption loops were formed. Hα observations from the Kanzelhöhe Solar Observatory further prove that this CME was related to a filament eruption, as can be seen in Figure 9*c*. Before the eruption, there was a dark, thick filament in the same region, and after the eruption it had gone.

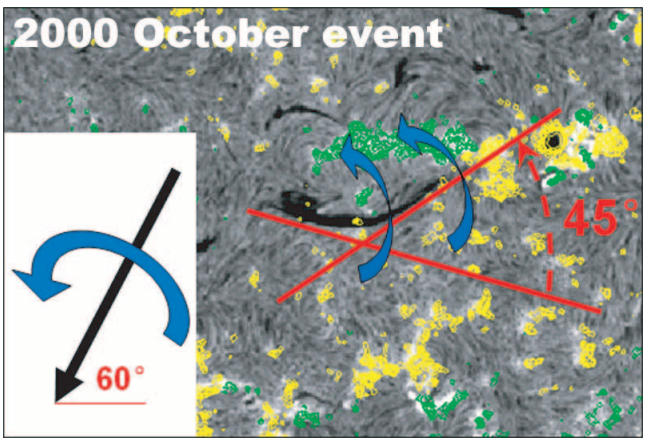

FIG. 7.—Same as Fig. 4, but for the 2000 October event.

Note that there was a minor CME that originated from the same region about half an hour earlier than the CME discussed above. It was slower and weaker than the earlier CME, and its angular width was $\sim 104^{\circ}$. Certainly one may also relate this minor CME to the November 20 MC. However, it does not affect our comparison between the MC and the filament, because the minor CME is associated with the same source region.

Using the same method to fit the observed MC, the fitted results are shown in the top three panels of Figure 8 and in Table 1. This MC possessed positive helicity, and its axis was in the direction of

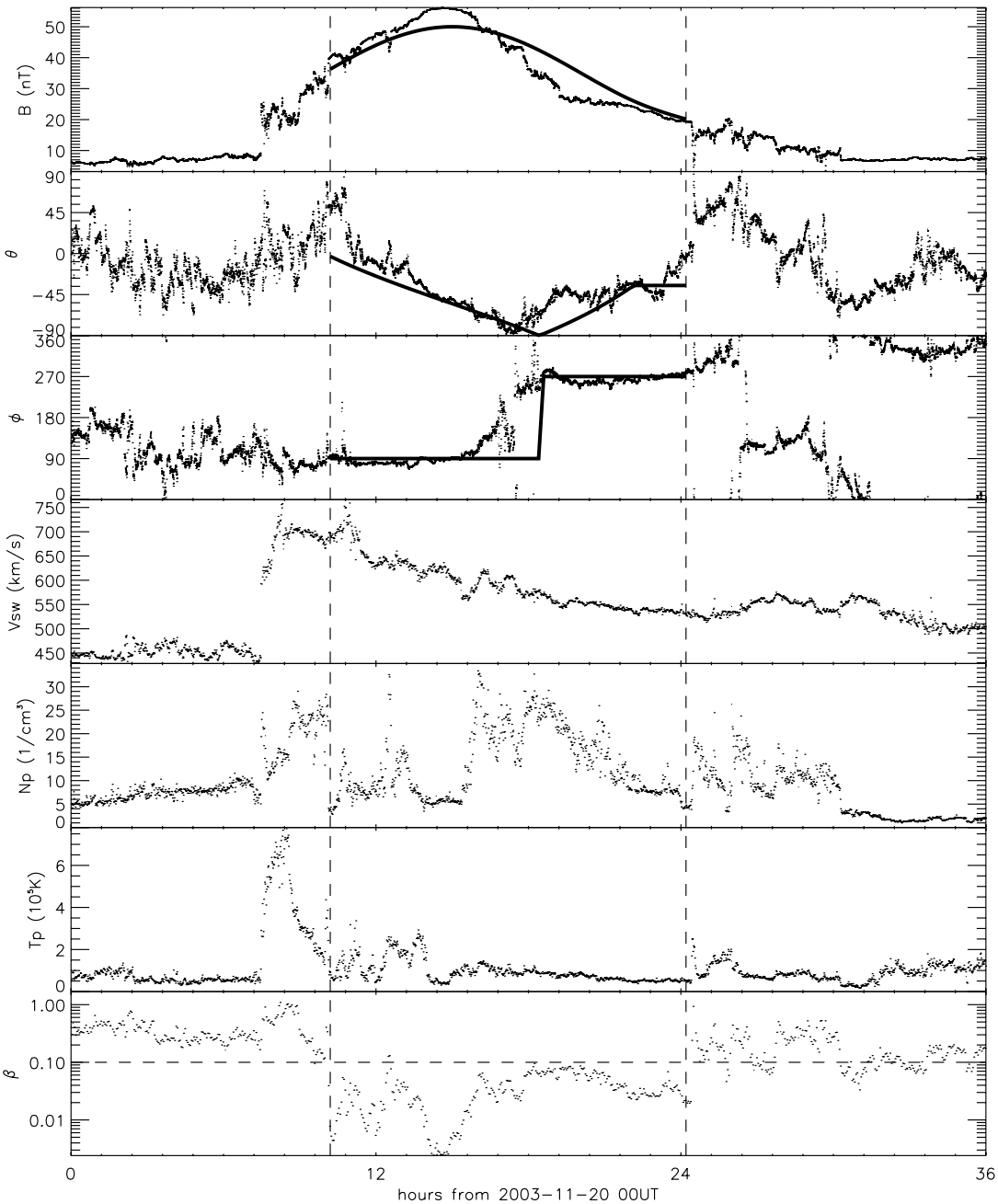

FIG. 8.—Same as Fig. 2, but for the 2003 November event.

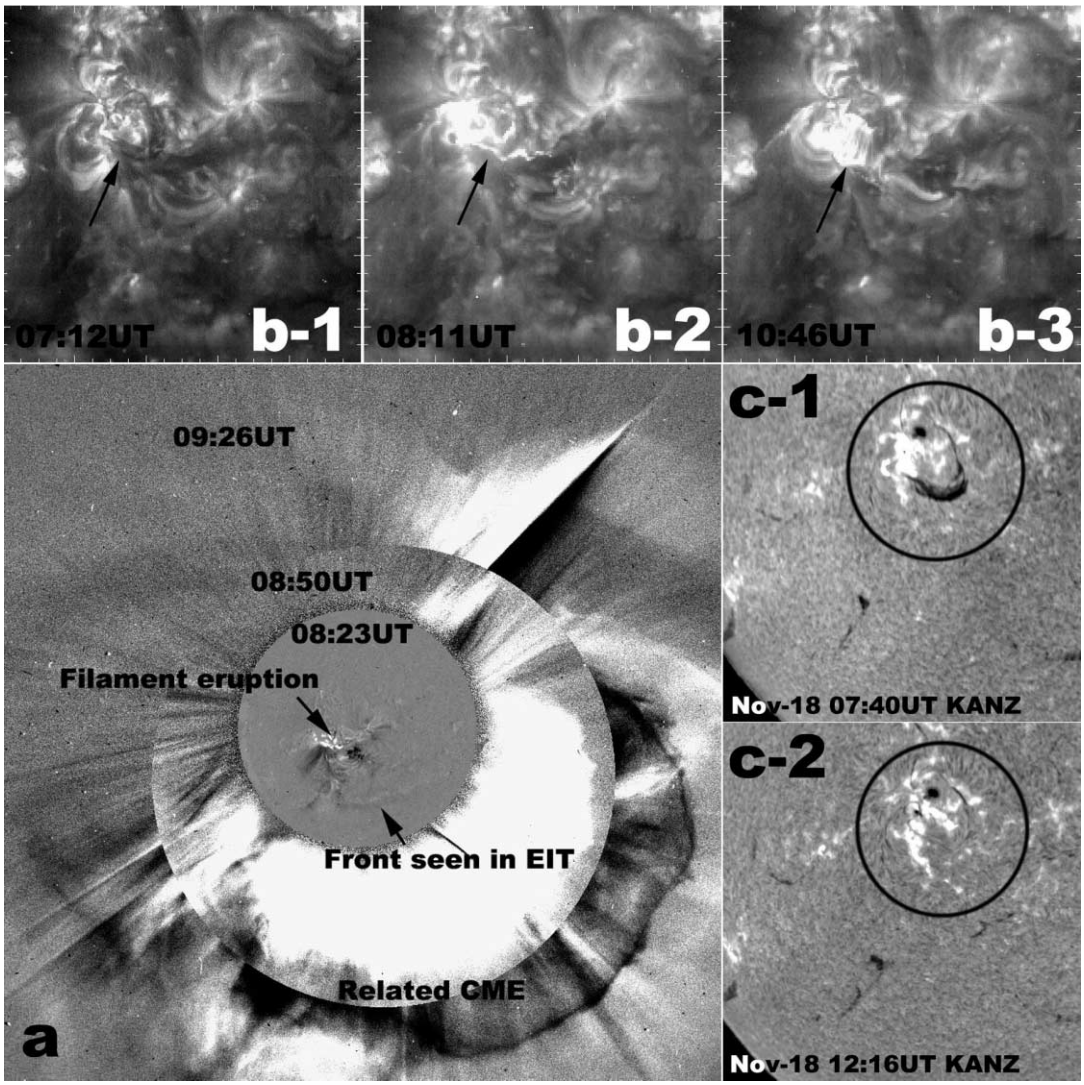

FIG. 9.—Same as Fig. 3, but for the 2003 November 18 CME and related solar activity.

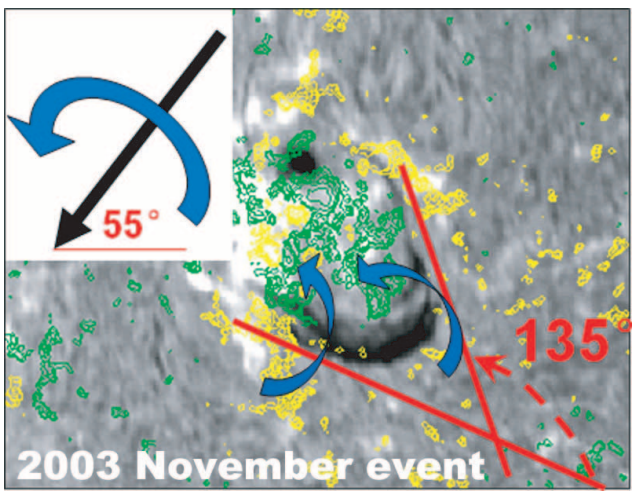

FIG. 10.—Same as Fig. 4, but for the 2003 November event.

$\theta \sim -55^\circ$ and $\phi \sim 90^\circ$, almost perpendicular to the Sun-Earth line. Thus, we expect that the leading front of this MC intersected Earth. From the values of θ and ϕ, the tilt angle of the MC axis is inferred to be $\sim 55^\circ$.

The associated filament was significantly curved from about -25° to 110°, spanning an angular range of 135° as shown in Figure 10. The estimated axial orientation of the MC is within this range and consistent with that of the central part of the filament. It should be noted that the posteruption loops only appeared on the east part of the erupted filament. It almost extended in the direction of -25° (as seen in Fig. 9*b*, *right*), which is significantly different from that of the MC axis. This fact suggests that such brightening loops may only appear in a compact region and not necessarily be centered beneath CMEs (Harrison 1986, 1995). The blue arrows in Figure 10 suggest that the direction of rotation of the helical magnetic field in the MC is consistent with that of the coronal field overlying the related filament.

3. SUMMARY AND DISCUSSION

The three filament-associated magnetic cloud events are summarized in Table 1. These three filaments are all significantly curved. In the first and third cases, the MC tilt angles are within the ranges of the tilt angles of the observed filaments, where

"range" is defined by tangents along the entire curved path of the filament, and almost parallel to the orientation of the central parts of the filaments. This result is consistent with many previous works, such as Bothmer & Schwenn (1994), Bothmer & Rust (1997), Marubashi (1997), McAllister et al. (2001), and Yurchyshyn et al. (2001). However, in the second case, the MC tilt angle is out of the range of the tilt angle of the associated filament. That is to say, the MC axis is not necessarily parallel to the original filament orientation. The deviation of the tilt angle between the MC and filament in that case implies that the correlation in orientation between MCs and their associated filaments prior to eruption may not be strong.

A preliminary effort to explain why the MC axis may not necessarily be parallel to the associated filament's orientation can be made by comparing the following two facts: (1) For both consistent events (the first and third), the estimated MC axes are nearly perpendicular to the Sun-Earth line, with angles of $\sim 75^\circ$ and $\sim 90^\circ$, respectively, which implies that the leading fronts of the two MCs are measured, based on the geometry (Fig. 1), and the projected MC axes almost align with the direction of the central parts of the associated filaments. (2) For the second event, the MC axis is not so perpendicular (angle $\sim 65^\circ$) to the Sun-Earth line, and its projection on the plane of the sky is out of the range of the filament orientation. These two contrasting differences hint that the consistency between MC axis and filament orientation probably depends on which part of the MC is detected. We therefore suggest that a correct prediction of MC axial orientation, with a small deviation from the orientation of an associated filament's long axis, might be made if the central part of the MC intersected Earth.

We examined all nine consistent cases presented in Marubashi (1997), in which the MC parameters were given. Based on Table 2 in that paper, the angles between the MC axes and the Sun-Earth line can be easily inferred. They were all larger than 45°. Two cases had angles larger than 50°, and six cases were larger than 70°. If an angle greater than 70° indicates a direction nearly perpendicular to the Sun-Earth line, that is, the leading front of the MC intersecting Earth, 6/9 of those cases follow the rule conjectured above. Certainly, we have to admit there is personal bias to claim a direction nearly perpendicular to the Sun-Earth line for angles larger than 70° and not for angles less than 70°. However, at least in our three cases, the inconsistent one has the smallest angle between the MC axis and the Sun-Earth line.

Thus, using observations of filaments and the surrounding magnetic fields to estimate the properties of resulting MCs and therefore predict subsequent geomagnetic storms is not as straightforward as was previously thought. In addition to the factor addressed in this paper, that the long axes of many filaments are highly curved, two additional factors, at least, need to be taken into account. First, CMEs are a large-scale phenomenon. They are not necessarily centered over the associated filaments, as pointed out by Harrison & Lyons (2000), Plunkett et al. (2001), etc. Second, the resulting MCs are an even larger scale structure. The average diameter of an MC at 1 AU is ~ 0.28 AU (Lepping et al. 1990). It is not known which part of the MC is observed, though the above preliminary analysis suggests that the leading front of an MC tends to align with the central part of its associated filament. Besides, the possible change in axial orientation of an MC when erupting and propagating through the corona and heliosphere is likely another factor. This may occur as a consequence of ambient solar wind or rotation of the MC. However, there is no direct evidence, although some numerical simulations have shown a significant rotation of CMEs (e.g., Fan & Gibson 2005). Maybe there are other factors, but the factors listed above do raise uncertainty in establishing the correlation between MC axis and filament orientation.

We acknowledge the use of solar data from the LASCO, EIT, and MDI instruments on board the *SOHO* spacecraft, interplanetary data from the *ACE* spacecraft, and Hα images from Kanzelhöhe Solar Observatory, BBSO, and YNAO. *SOHO* is a project of international cooperation between ESA and NASA. We thank the anonymous referee for many constructive suggestions and criticisms. We also thank Jie Zhang, Arthur I. Poland, and Oscar A. Olmedo for comments and proofreading. This work was supported by grants from the National Natural Science Foundation of China (40525014, 40404014, 40336052, 40336053), the 973 Project (2006CB806304), and the Chinese Academy of Sciences (KZCX3-SW-144 and Startup Fund).

REFERENCES

Berdichevsky, D. B., Richardson, I. G., Lepping, R. P., & Martin, S. F. 2005, J. Geophys. Res., 110, No. A09105
Bothmer, V., & Rust, D. M. 1997, in Coronal Mass Ejections, ed. N. Crooker, J. A. Joselyn, & J. Feynman (Washington: Am. Geophys. Union), 139
Bothmer, V., & Schwenn, R. 1994, Space Sci. Rev., 70, 215
Brueckner, G. E., et al. 1995, Sol. Phys., 162, 357
Burlaga, L., Sittler, E., Mariani, F., & Schwenn, R. 1981, J. Geophys. Res., 86, 6673
Burlaga, L. F. 1988, J. Geophys. Res., 93, 7217
Burlaga, L. F., Skoug, R. M., Smith, C. W., Webb, D. F., Zurbuchen, T. H., & Reinard, A. 2001, J. Geophys. Res., 106, 20957
Burton, R. K., McPherron, R. L., & Russell, C. T. 1975, J. Geophys. Res., 80, 4204
Cane, H. V., Richardson, I. G., & Wibberenz, G. 1997, J. Geophys. Res., 102, 7075
Cliver, E. W., Feynman, J., & Garrett, H. B. 1990, J. Geophys. Res., 95, 17103
Delaboudinière, J.-P., et al. 1995, Sol. Phys., 162, 291
Ermolaev, Yu. I., et al. 2005, Geomagn. Aeron., 45, 20
Fan, Y., & Gibson, S. E. 2005, in Connecting Sun and Heliosphere, ed. B. Flack, T. H. Zurbuchen, & H. Lacoste (ESA SP-592; Noordwijk: ESA), 241
Farrugia, C. J., Burlaga, L. F., Osherovich, V. A., Richardson, I. G., Freeman, M. P., Lepping, R. P., & Lazarus, A. J. 1993, J. Geophys. Res., 98, 7621
Filippov, B. P. 1998, in IAU Colloq. 167, New Perspectives on Solar Prominences, ed. D. Webb, D. Rust, & B. Schmieder (ASP Conf. Ser. 150; San Francisco: ASP), 342
Goldstein, H. 1983, in Solar Wind Five, ed. M. Neugebauer (NASA CP-2280; Washington: NASA), 731
Gonzalez, W. D., & Tsurutani, B. T. 1987, Planet. Space Sci., 35, 1101
Gonzalez, W. D., Tsurutani, B. T., Gonzalez, A. L. C., Smith, E. J., Tang, F., & Akasofu, S.-I. 1989, J. Geophys. Res., 94, 8835
Gosling, J. T., Birn, J., & Hesse, M. 1995, Geophys. Res. Lett., 22, 869
Gosling, J. T., McComas, D. J., Phillips, J. L., & Bame, S. J. 1991, J. Geophys. Res., 96, 7831
———. 1992, J. Geophys. Res., 97, 6531
Harrison, R. A. 1986, A&A, 162, 283
———. 1995, A&A, 304, 585
Harrison, R. A., & Lyons, M. 2000, A&A, 358, 1097
Hudson, H. S., Lemen, J. R., St. Cyr, O. C., Sterling, A. C., & Webb, D. F. 1998, Geophys. Res. Lett., 25, 2481
Jing, J., Yurchyshyn, V. B., Yang, G., Xu, Y., & Wang, H. 2004, ApJ, 614, 1054
Kumar, A., & Rust, D. M. 1996, J. Geophys. Res., 101, 15667
Lepping, R. P., Jones, J. A., & Burlaga, L. F. 1990, J. Geophys. Res., 95, 11957
Lundquist, S. 1950, Ark. Fys., 2, 361
Martin, S. F., & McAllister, A. H. 1997, in Coronal Mass Ejections, ed. N. Crooker, J. A. Joselyn, & J. Feynman (Washington: Am. Geophys. Union), 127
Marubashi, K. 1997, in Coronal Mass Ejections, ed. N. Crooker, J. A. Joselyn, & J. Feynman (Washington: Am. Geophys. Union), 147
McAllister, A. H., Martin, S. F., Crooker, N. U., Lepping, R. P., & Fitzenreiter, R. J. 2001, J. Geophys. Res., 106, 29185
Perreault, P., & Akasofu, S.-I. 1978, Geophys. J., 54, 547
Plunkett, S. P., Thompson, B. J., St. Cyr, O. C., & Howard, R. A. 2001, J. Atmos. Sol.-Terr. Phys., 63, 389
Richardson, I. G., & Cane, H. V. 2004, Geophys. Res. Lett., 31, No. L18804

Rust, D. M., Anderson, B. J., Andrews, M. D., Acuña, M. H., Russell, C. T., Schuck, P. W., & Mulligan, T. 2005, ApJ, 621, 524
Sheeley, N. R., Jr., Howard, R. A., Koomen, M. J., Michels, D. J., Schwenn, R., Mühlhäuser, K.-H., & Rosenbauer, H. 1985, J. Geophys. Res., 90, 163
Tsurutani, B. T., & Gonzalez, W. D. 1995, J. Atmos. Terr. Phys., 57, 1369
Wang, Y., Shen, C., Wang, S., & Ye, P. 2004, Sol. Phys., 222, 329
Wang, Y., Shen, C.-L., Wang, S., & Ye, P.-Z. 2003a, Geophys. Res. Lett. 30(20), No. 2039
Wang, Y., Xue, X., Shen, C., Ye, P., Wang, S., & Zhang, J. 2006, ApJ, 646, 625
Wang, Y.-M., Wang, S., & Ye, P.-Z. 2002a, Sol. Phys., 211, 333
Wang, Y.-M., Ye, P.-Z., & Wang, S. 2003b, J. Geophys. Res., 108(A10), No. 1370
Wang, Y.-M., Ye, P.-Z., Wang, S., Zhou, G.-P., & Wang, J.-X. 2002b, J. Geophys. Res., 107(A11), No. 1340
Yurchyshyn, V. B., Wang, H., Goode, P. R., & Deng, Y. 2001, ApJ, 563, 381